Letter

Effective temperature and dissipation of a gas of active particles probed by the vibrations of a flexible membrane

Jean François Boudet, Julie Jagielka, Thomas Guerin, Thomas Barois, Fabio Pistolesi, and Hamid Kellay
Université de Bordeaux, CNRS LOMA UMR 5798, Talence F-33405, France

(Received 17 February 2022; accepted 7 September 2022; published 10 October 2022)

We use a flexible circular membrane to probe a gas of macroscopic self-propelled rod-like robots. The fluctuations of the membrane are completely described by a set of discrete modes with different characteristic frequencies. We show that the dynamics of each mode can be well described by a Langevin equation with a white noise and a frequency-independent dissipation. This allows to extract the dissipation and fluctuation intensity for each mode, and consequently the contribution to the dissipation due to the collisions with the gas. The ratio of the gas-generated fluctuation and dissipation does not depend on the mode, indicating that the system interacts with the membrane as an equilibrium environment at a given effective temperature. We also find that this effective temperature coincides with the average kinetic energy of the rod-like robots. Quite surprisingly, this study thus shows that in a wide range of densities and frequencies the behavior of self-propelled robots can be regarded as that of an equilibrium gas. The method is quite general, and can be used to unveil deviations from this simple behavior in other regimes.

DOI: 10.1103/PhysRevResearch.4.L042006

An ensemble of active entities with minimal ingredients (self-locomotion, simple configurational change,...) can display complex behavior such as global organization and abilities that may go beyond those of the individual particles [1–11]. Such features and others make active matter attractive for a range of applications going from new materials to biology and robotics [12–16]. Different types of entities have been used from motile vibrating bots, colloidal active particles, to shape changing and/or light sensitive particles [2–5,7,8,17,18].

Yet, and despite a number of studies on their self-organization in bulk and under confinement using diverse objects spanning a wide range of scales [4,19–28], it remains a fundamental challenge to predict macroscopic properties such as the pressure, the effect of boundaries, or the identification of a quantity that could play the role of a temperature of such assemblies [5,10,29–40]. Strictly speaking, the temperature can only be defined in equilibrium systems. Whether active matter can be described as a system at thermal equilibrium is nontrivial. The concept of effective temperature in active matter [32,34] or vibrated granular beds [41] can have drawbacks and may depend on the time scale [42–44] but may also be subject to spatial inhomogeneity due to phase separation or long-lived giant fluctuations [4,20,23,32].

Consider the case of a gas of active particles. From the experimental point of view one could investigate the statistical properties of the gas itself. A different attitude is to put the system in contact with another system, a probe, and study how that system behaves. In general the gas of particles will exchange energy and momentum with the probe. In equilibrium, the dissipation and the fluctuating disturbance acting on the probe are related by the fluctuation-dissipation theorem [45] with their ratio being proportional to the temperature of the gas. For a system out of equilibrium the dissipation and the fluctuations can be completely independent, and thus depend on the physical quantity or conditions considered. Thus the investigation of the relation between the fluctuation and the dissipation can bring crucial information on the behavior of an active particle gas.

Here, we report experimental work showing that the dissipation and fluctuation spectrum generated by a gas of active particles interacting with a vibrating membrane can be related by the dissipation-fluctuation relation, allowing the definition of an effective temperature for the membrane $T^m_{\rm eff}$ and for the gas $T^G_{\rm eff}$. These two temperatures turn out to be different with the membrane temperature having a dependence on both mode number and surface fraction of particles. However, we found that $T^G_{\rm eff}$ is independent of density and of the spatial, and temporal scale of the measurements. To achieve this result, we have measured simultaneously the dissipation and the fluctuation intensity. The existence of this relation does not necessarily imply that the system is actually in equilibrium, but it clearly gives important information on its behavior.

We use a circular, but flexible membrane surrounded by active particles. The membrane and particles are in ambient air with negligible interactions due to the ambient medium as its density and viscosity are very low. As the active particles collide randomly with the membrane, they excite its mechanical modes whose amplitudes fluctuate in time. The active particles are self-propelled rods with sufficient inertia that aggregation occurs only at high enough densities near

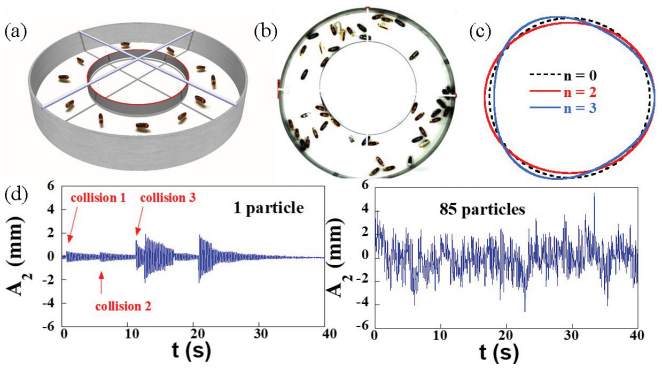

FIG. 1. (a) Experimental setup: an inner flexible circle is suspended by four thin wires fixed to the upper cross surrounded by an empty area delimited by the outer arena. (b) Photograph of the experiment where $N = 45$ rod like robots are inserted in the empty area between inner and outer rings. (c) Schematic of the different deformation modes of the circular flexible membrane. (d) Amplitude of the second mode ($n = 2$) of membrane fluctuations for $N = 1$ and $N = 85$ particles. $R = 30$ cm, $r_0 = 16$ cm, $e = 200$ μm.

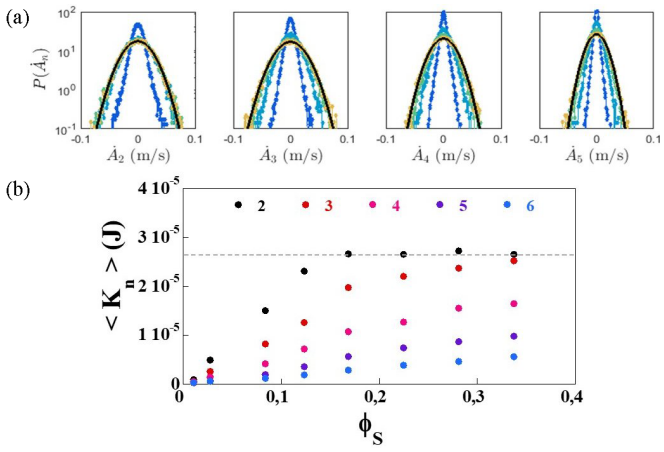

FIG. 2. (a) pdfs of velocity fluctuations for different modes n and varying ϕ_S: 0.03 (blue), 0.12 (cyan), 0.23 (green) 0.34 (yellow). The black line is a Gaussian fit. (b) Effective energy $\langle K_n \rangle$ from velocity fluctuations for different n versus ϕ_S. $R = 24$ cm, $r_0 = 16$ cm, $e = 550$ μm. The dashed line indicates the plateau value.

boundaries [5]: When confined in rigid circular arenas, dilute assemblies of such rods act as a gas. Increasing the surface fraction leads to collective behavior near the boundaries with the emergence of polar clusters while, in the bulk, gas-like behavior persists. The phase diagram for the transition from gas-like behavior to a coexistence region between a gas and surface clusters was established in [5] and is a direct consequence of inertial effects. The experiments carried out here concern primarily the gas phase region of this phase diagram. To examine membrane fluctuations, in a two-dimensional setup, friction of the membrane with the supporting surface needs to be minimized. Here, the membrane was suspended by four wires a few millimeters above the surface so that in the absence of particles, dissipation is only due to air drag.

The plastic electromechanical rod-like robots are 4.5 cm in length, 2 cm in height, and 1.5 cm in width with a mass m of 7 g. Their mobility is induced by the vibration of the robot itself which is equipped with a vibration module, driven by an embedded battery, working at frequencies near 100 Hz. These rods have asymmetric soft legs, which allow directed movement with velocities that can reach $V = 30$ cm/s [5,46]. We confine a number N of active rods in a fixed rigid circular arena of radius R. In the central area, we insert another circular membrane which consists of a thin stainless steel strip of width $h = 2$ cm, of different thicknesses e and of radius r_0 smaller than R.

There are no robots inside the membrane so that the robots are confined to the space between the outer arena and the central membrane with a surface fraction $\phi_S = Na/s$; a and s are the projected area of the rods and the total area accessible to them. The radius R was varied from 20 cm to 30 cm, r_0 was 16 cm while different values of e (100, 200, 250, and 550 μm) were used. The variation of these parameters allows to vary the resonance frequencies of the membrane, its inherent dissipation and mass, as well as the surface fraction of particles. The setup, Fig. 1(a), is visualized from above with a fast camera; a photograph of the experiment is shown in Fig. 1(b). The collisions of the active rods with the flexible membrane excite its vibrations which come in several modes n (see Fig. 1(c)). These vibrations are measured, via image analysis, with a temporal resolution of 250 Hz (see Supplemental Material [47]). From the time series of the membrane fluctuations, we isolate the amplitude of the different modes of vibration by decomposing the distance $r(\theta, t)$ to the membrane center into Fourier modes, which turn out to be also the eigenmodes of the membrane fluctuations:

$$r(\theta, t) = r_0 + \sum_{n \geqslant 1} A_n^+(t)\cos(n\theta) + A_n^-(t)\sin(n\theta). \qquad (1)$$

θ designates the angular position along the membrane. Examples of signals $A_n^+(t)$ are shown in Fig. 1(d) for $n = 2$. For $N = 1$, the collisions with the membrane are visible as impulses with a characteristic frequency and a decay time. For $N = 85$, the signal resembles a random time series. Fourier analysis of these vibrations which are then averaged over time gives access to the spectral properties of the fluctuations for any mode n.

We first examine the energy content of the fluctuations of the membrane. The probability density functions (pdf) of the velocity fluctuations $\dot{A}_n$ (the pdfs for $\dot{A}_n^+$ and $\dot{A}_n^-$ are similar so we drop the signs in the following) for different modes n and different ϕ_S are shown in Fig. 2(a). The widths of the pdfs increase as ϕ_S increases while the pdfs become gradually Gaussian at higher ϕ_S (see Fig. S1 in the Supplemental Material [47]). We show in [47] that the kinetic energy of the membrane can be written as $E_k = \sum_n M_n[(\dot{A}_n^+)^2 + (\dot{A}_n^-)^2]/2$, where $M_n = \frac{n^2+1}{2n^2}M$ is a modal mass. This suggests to define $\langle K_n \rangle = M_n \langle \dot{A}_n^2 \rangle$ as a measure of the effective kinetic energy for mode n, which can be obtained from the squared width of the pdfs of $\dot{A}_n$. The brackets denote an average over time, equivalent to ensemble averaging for long enough signals. This energy is plotted in Fig. 2(b) for different n versus ϕ_S. For low ϕ_S, $\langle K_n \rangle$ increases fast before saturation. This is particularly true for $n = 2$ and $n = 3$. When mode 2 saturates at some ϕ_S, mode 3 saturates at a higher value, and mode 4, does not at the accessible ϕ_S. If the membrane were at equilibrium

at temperature T, all $\langle K_n \rangle$ would be equal to $k_B T$ which is clearly not the case.

To shed light on this behavior, the interplay between membrane fluctuations and the collisions with the gas particles needs to be examined. We model the dynamics of membrane fluctuations by considering the membrane as an inextensible two-dimensional elastic strip [48] subjected to dissipation, proportional to the local velocity of the membrane, and to external random forces due to collisions with active robots. If the membrane deformation is small enough to consider the linearized dynamics around a perfect circle, the equation for the dynamics of each mode takes the form

$$\ddot{A}_n + 2\gamma_n(\phi_S)\,\dot{A}_n + \omega_n^2\,A_n = F_n, \tag{2}$$

where F_n is a combination of the perpendicular and parallel components of the forces exerted by the colliding robots, rescaled by the mass of the membrane (see Supplemental Material [47]). The equations for A_n^+ and A_n^- are similar, upon replacing F_n by F_n^+ or F_n^-. Here, we assume that the membrane elasticity governs the membrane dynamics and that the dissipation is a simple function of the local velocity but with a rate $\gamma_n(\phi_S)$ which depends on ϕ_S.

The resonance frequencies of the different modes are given by $\omega_n^2 = \frac{(n^2-1)^2\pi\kappa}{M_n r_0^3}$. Here, $\kappa = \frac{Ee^3h}{12(1-\nu)^2}$ is the bending modulus of the membrane strip with E the Young modulus and ν the Poisson ratio. Note that Eq. (2) is not a standard Langevin equation since the random forcing $F_n(t)$ on the right-hand side may take the form of a discrete series of impulses, giving rise to non-Gaussian pdfs for A_n, as in the examples of Fig. 2(a). Nevertheless, the equation for A_n, when Fourier transformed relates the power spectrum of the velocity fluctuations of the membrane to that of the noise due to random collisions with the robots [49]:

$$S_{\dot{A}_n}(\omega) = \frac{\omega^2\, S_{F_n}(\omega)}{\left(\omega^2 - \omega_n^2\right)^2 + [2\gamma_n(\phi_S)\omega]^2}. \tag{3}$$

The power spectral density $S_X(\omega)$ for any stationary random signal $X(t)$ is defined such that $\langle \hat{X}(\omega)\hat{X}(\omega')\rangle = 4\pi^2\delta(\omega + \omega')S_X(\omega)$, where $\hat{X}(\omega) = \int_{-\infty}^{\infty} dt X(t)e^{-i\omega t}$ is the Fourier transform of $X(t)$.

Power spectra of the velocity fluctuations for up to $n = 5$ are shown in Fig. 3(a). Each mode shows a well defined peak at a well-defined resonance frequency with a well-defined width. The spectra of Fig. 3(a) are well described by [Eq. (3)], using a noise spectrum $S_{F_n}(\omega)$ independent of ω, suggesting that this noise is temporally uncorrelated as assumed in our theoretical analysis detailed in SI. From such fits, the values of ω_n and $\gamma_n(\phi_S)$ can be obtained. The ω_n follow the expected behavior (see Fig. S2 in the Supplemental Material [47]) while the dissipation depends on n and increases with ϕ_S as shown in Fig. 3(b). This increase is roughly the same for different modes (from 2 to 5), with a non zero intercept as ϕ_S goes to zero. This intercept, which is mode dependent, is the dissipation in the absence of rods $\gamma_n^{\rm air}$ which increases with n, similarly to the dissipation due to air of a linear strip with similar dimensions (see Fig. S3 in the Supplemental Material [47]), pointing to the origin of this dissipation as being due to air drag [50]. An interesting finding is the additive nature of the dissipation from air drag and that from the presence of the active gas which allows to disentangle them properly:

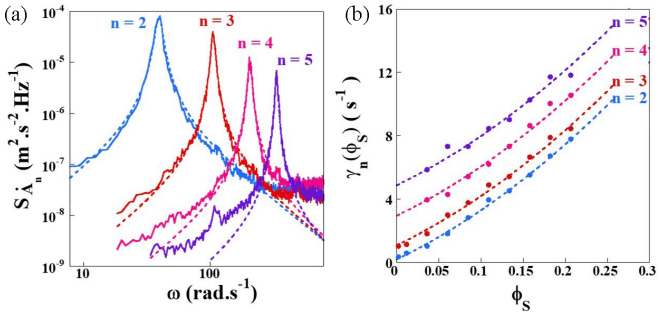

FIG. 3. (a) Power spectrum of velocity fluctuations for the different modes n of the membrane. The dashed lines are fits to the theoretical spectrum from the Langevin equation. $\phi_S = 0.1$, $R = 24$ cm, $r_0 = 16$ cm, $e = 250$ μm. (b) Dissipation parameter for different modes versus ϕ_S, $R = 30$ cm, $r_0 = 16$ cm, $e = 200$ μm. The dashed lines are guides to the eye.

$$\gamma_n(\phi_S) = \gamma(\phi_S) + \gamma_n^{\rm air}. \tag{4}$$

The dissipation from the gas of active particles $\gamma(\phi_S)$ increases with ϕ_S and is independent of n. In addition, the fits suggest strongly that $\gamma(\phi_S)$ is independent of ω. One can now introduce an effective temperature for the membrane $T_{\rm eff}^m$ using $S_{F_n}(\omega) = \frac{2}{\pi M_n}\gamma_n(\phi_S)k_B T_{\rm eff}^m$ as in the fluctuation dissipation theorem with k_B the Boltzmann constant. This effective temperature is directly related to the kinetic energy of the nth mode of the membrane $\langle K_n \rangle = k_B T_{\rm eff}^m$ (see [47]).

These measurements show that the characteristic energy $\langle K_n \rangle$ and thus the effective temperature of the membrane depend on the surface fraction. In order to understand this dependence, we have examined how the different effective energies from different modes and for different values of ϕ_S can be rescaled. The problem at hand has two characteristic time scales. The first one is simply the dissipation time scale. The second is the inverse of the frequency of collisions of the robots with the membrane f_c. This frequency naturally depends on the surface fraction and, from our estimates, varies roughly linearly with ϕ_S, at least at low surface fractions (see Fig. S4 in the Supplemental Material [47]). We plot in Fig. 4 $\langle K_n \rangle$ for different modes n and densities ϕ_S versus the ratio: $f_c/\gamma_n(\phi_S)$. This rescaling versus a nondimensional quantity collapses, fairly well, $\langle K_n \rangle$ on a single curve, for data from different runs with different densities and membrane properties.

The characteristic energy or effective temperature of the membrane becomes constant, independent of ϕ_S and n, only when f_c becomes higher than the total dissipation rate $\gamma_n(\phi_S)$. The plateau value of this characteristic energy turns out to be independent of the membrane properties (see Fig. S5 in the Supplemental Material [47]) and is characteristic of the gas of particles as it varies roughly linearly with the kinetic energy of the particles (see Fig. S5 in the Supplemental Material [47]).

Now, consider the dissipation due to the gas of particles. If we consider the membrane as a large particle surrounded by a gas of smaller ones, dissipation can be traced to the inelastic nature of the collisions of the membrane with the active particles. The dissipated power is proportional to the number of collisions per unit time, or f_c.

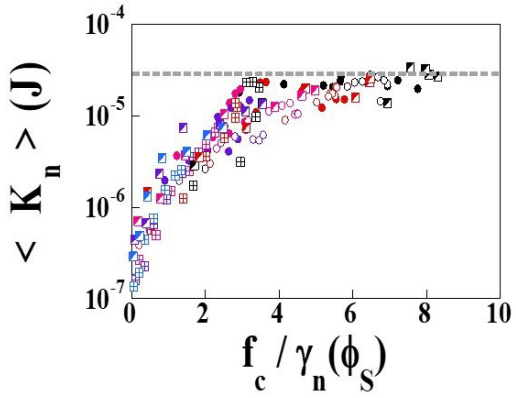

FIG. 4. $\langle K_n \rangle$ for different modes and different membranes versus the ratio of frequency of collisions to dissipation rate. $r_0 = 16$ cm, $(e, R) = (100\ \mu$m, 30 cm), (200 μm, 30 cm), (250 μm, 20 cm), and (550 μm, 24 cm). The dashed lines indicate the plateau value. The colors indicate different mode numbers: black $n = 2$, red $n = 3$, violet $n = 5$, blue $n = 6$.

Thus $\gamma(\phi_S)$ should be proportional to f_c as borne out by experiments, Fig. 5(a).

Both the dissipation due to the gas and the effective energy of the membrane depend on ϕ_S via the collision frequency f_c. But so far, whether the gas of active particles has a well defined effective temperature and how it is related to the effective temperature of the membrane has not been considered. The membrane is subject to both noise and dissipation from the active bath but also from the surrounding air. The driving noise is solely due to the active gas as the effect of the ambient air is negligible, but both environments contribute to the dissipation. The effective temperature $T^G_{\rm eff}$ of the gas is then linked in a straightforward manner to the effective temperature of the membrane. The relation between the two, as for a classical oscillator subjected to two different sources of noise and dissipation [51,52], is given by $\gamma_n(\phi_S)T^m_{\rm eff} = \gamma_n^{\rm air} T + \gamma(\phi_S)T^G_{\rm eff}$.

A way to see the variation of $T^m_{\rm eff}$ with ϕ_S is to regard it as if it is coupled to two reservoirs, one at practically vanishing temperature (the air) and the other at $T^G_{\rm eff}$ (the gas). The resulting temperature $T^m_{\rm eff}$ of the membrane is then given by the weighted average of the two, with the weights given by the ratio of the couplings that is the ratio of the dissipation to the total dissipation. Since the ambient temperature T is orders of magnitude smaller than that of the membrane, we obtain $T^G_{\rm eff} = \frac{\gamma_n^{\rm air}+\gamma(\phi_S)}{\gamma(\phi_S)} T^m_{\rm eff}$. Figure 5(b) shows that $T^G_{\rm eff}$ is independent of n (inset of Fig. 5(b) and ϕ_S; its value corresponds to the plateau value of $\langle K_n \rangle$. The effective temperature of the gas is thus similar for different membrane thicknesses and radii and is solely determined by the kinetic energy of the active robots. Thus, the gas of active robots has a well-defined effective temperature.

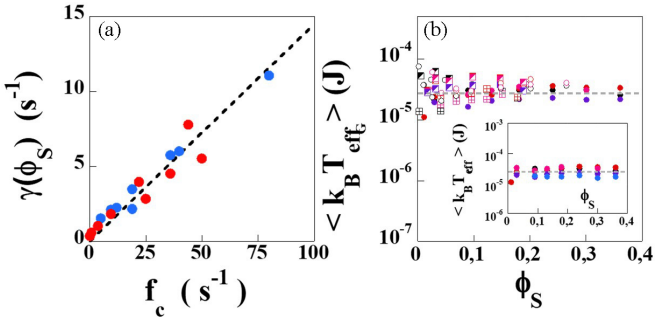

FIG. 5. (a) Dissipation due to the gas of particles only versus frequency of collisions. The dashed line shows a linear dependence. (blue symbols: $e = 250\ \mu$m, red symbols: $e = 200\ \mu$m). (b) Effective energy of the gas of active particles versus ϕ_S for the same data as in Fig. 4. Inset: Effective energy of the gas versus ϕ_S for $r_0 = 16$ cm, (e, R)= (550 μm, 24 cm). The colors indicate mode number as in Fig. 4. The dashed lines indicate the plateau value of the effective energy.

The system we use is one of a few where statistical mechanics techniques can be used to extract quantities that are difficult to access in most experiments. The fact that the dissipation as well as the effective temperature can be retrieved in a reliable way in an active system is itself remarkable. It is only by carrying out a detailed analysis that an effective temperature of the gas could be extracted. Note that if we had analyzed only the membrane fluctuations (such as the pdfs of Fig. 2(a)) without a detailed theoretical analysis, a detailed analysis of the spectral structure as well as the measurement of the dissipation, we could have reached the wrong conclusion: that the temperature of the system is ill defined (see our Fig. 2(b). It is only by disentangling the different contributions (ambient medium, and active gas) to the dissipation that we were able to extract correct information. Few if any active systems have been shown to exhibit a well defined effective temperature. That the techniques used and the system chosen allow this is in itself a remarkable finding. That this property may break down under different conditions does not reduce the scope of our results. On the contrary, one can use the tools developed here to analyze the reasons for break down in more complex systems in detail.

To conclude, two salient features characterize the gas of active rod like robots. First, the dissipation rate of the probe membrane, due to this gas, depends on the surface fraction of the particles in a way close to how a large granular particle surrounded by smaller ones dissipates energy through collisions. Second, the effective temperature of this gas turns out to be independent of mode number, membrane properties, and surface fraction. It is thus well defined and is determined solely by the properties of the robots themselves: it coincides with the average kinetic energy of the particles. The results are of importance for active matter, a nonequilibrium system, showing experimentally that an active gas such as ours is ideal and its action on a probe (the membrane) can be described by equilibrium like properties and thus a simple Langevin equation with a white noise and frequency independent dissipation. We anticipate that deviations from this behavior will arise when clusters, aggregates, or other collective effects emerge. The tools developed here can bring valuable insight in such a case.

This work was partially funded by Institut Universitaire de France. We thank J. Lintuvuori for discussions and R. Houques for help with the experimental setup.

[1] T. Vicsek and A. Zafeiris, Collective motion, Phys. Rep. **517**, 71 (2012).

[2] C. Bechinger, R. Di Leonardo, H. Löwen, C. Reichhardt, G. Volpe, and G. Volpe, Active particles in complex and crowded environments, Rev. Mod. Phys. **88**, 045006 (2016).

[3] G. Popkin, The physics of life, Nature (London) **529**, 16 (2016).

[4] A. Bricard, J. B. Caussin, N. Desreumaux, O. Dauchot, and D. Bartolo, Emergence of macroscopic directed motion in populations of motile colloids, Nature (London) **503**, 95 (2013).

[5] A. Deblais, T. Barois, T. Guerin, P. H. Delville, R. Vaudaine, J. S. Lintuvuori, J. F. Boudet, J. C. Baret, and H. Kellay, Boundaries Control Collective Dynamics of Inertial Self-Propelled Robots, Phys. Rev. Lett. **120**, 188002 (2018).

[6] J.-F. Boudet, J. Lintuvuori, C. Lacouture, T. Barois, A. Deblais, K. Xie, S. Cassagnere, B. Tregon, D. Brückner, J.-C. Baret *et al.*, From collections of independent, mindless robots to flexible, mobile, and directional superstructures, Science Robotics **6**, eabd0272 (2021).

[7] S. Li, R. Batra, D. Brown, H. D. Chang, N. Ranganathan, C. Hoberman, D. Rus, and H. Lipson, Particle robotics based on statistical mechanics of loosely coupled components, Nature (London) **567**, 361 (2019).

[8] W. Savoie, T. A. Berrueta, Z. Jackson, A. Pervan, R. Warkentin, S. Li, T. D. Murphey, K. Wiesenfeld, and D. I. Goldman, A robot made of robots: Emergent transport and control of a smarticle ensemble, Science Robotics **4**, eaax4316 (2019).

[9] S. Li, B. Dutta, S. Cannon, J. J. Daymude, R. Avinery, E. Aydin, A. W. Richa, D. I. Goldman, and D. Randall, Programming active cohesive granular matter with mechanically induced phase changes, Sci. Adv. **7**, eabe8494 (2021).

[10] M. Paoluzzi, R. Di Leonardo, M. C. Marchetti, and L. Angelani, Shape and displacement fluctuations in soft vesicles filled by active particles, Sci. Rep. **6**, 34146 (2016).

[11] C. Abaurrea-Velasco, T. Auth, and G. Gompper, Vesicles with internal active filaments: self-organized propulsion controls shape, motility, and dynamical response, New J. Phys. **21**, 123024 (2019).

[12] M. Sitti, Bio-inspired robotic collectives, Nature (London) **567**, 314 (2019).

[13] P. Fischer, A machine from machines, Nat. Phys. **14**, 1072 (2018).

[14] M. Rubenstein, A. Cornejo, and R. Nagpal, Programmable self-assembly in a thousand-robot swarm, Science **345**, 795 (2014).

[15] J. C. Barca and Y. A. Sekercioglu, Swarm robotics reviewed, Robotica **31**, 345 (2013).

[16] B. Vincenti, G. Ramos, M. L. Cordero, C. Douarche, R. Soto, and E. Clément, Magnetotactic bacteria in a droplet self-assemble into a rotary motor, Nat. Commun. **10**, 5082 (2019).

[17] T. Barois, J.-F. Boudet, J. S. Lintuvuori, and H. Kellay, Sorting and Extraction of Self-Propelled Chiral Particles by Polarized Wall Currents, Phys. Rev. Lett. **125**, 238003 (2020).

[18] J. Aguilar, T. Zhang, F. Qian, M. Kingsbury, B. McInroe, N. Mazouchova, C. Li, R. Maladen, C. Gong, M. Travers *et al.*, A review on locomotion robophysics: The study of movement at the intersection of robotics, soft matter and dynamical systems, Rep. Prog. Phys. **79**, 110001 (2016).

[19] D. Saintillan and M. J. Shelley, Theory of Active Suspensions, in *Complex Fluids in Biological Systems* (Springer, Berlin, 2015), pp. 319–355.

[20] F. Peruani, Active Brownian rods, Eur. Phys. J.: Spec. Top. **225**, 2301 (2016).

[21] G. A. Patterson, P. I. Fierens, F. Sangiuliano Jimka, P. G. König, A. Garcimartín, I. Zuriguel, L. A. Pugnaloni, and D. R. Parisi, Clogging Transition of Vibration-Driven Vehicles Passing through Constrictions, Phys. Rev. Lett. **119**, 248301 (2017).

[22] T. Barois, J. F. Boudet, N. Lanchon, J. S. Lintuvuori, and H. Kellay, Characterization and control of a bottleneck-induced traffic-jam transition for self-propelled particles in a track, Phys. Rev. E **99**, 052605 (2019).

[23] V. Narayan, S. Ramaswamy, and N. Menon, Long-lived giant number fluctuations in a swarming granular nematic, Science **317**, 105 (2007).

[24] I. Theurkauff, C. Cottin-Bizonne, J. Palacci, C. Ybert, and L. Bocquet, Dynamic Clustering in Active Colloidal Suspensions with Chemical Signaling, Phys. Rev. Lett. **108**, 268303 (2012).

[25] E. Lushi, H. Wioland, and R. E. Goldstein, Fluid flows created by swimming bacteria drive self-organization in confined suspensions, Proc. Natl. Acad. Sci. USA **111**, 9733 (2014).

[26] Y. Alapan, O. Yasa, O. Schauer, J. Giltinan, A. F. Tabak, V. Sourjik, and M. Sitti, Soft erythrocyte-based bacterial microswimmers for cargo delivery, Science Robotics **3**, eaar4423 (2018).

[27] C. Scholz, S. Jahanshahi, A. Ldov, and H. Löwen, Inertial delay of self-propelled particles, Nat. Commun. **9**, 5156 (2018).

[28] O. Dauchot and V. Démery, Dynamics of a Self-Propelled Particle in a Harmonic Trap, Phys. Rev. Lett. **122**, 068002 (2019).

[29] M. C. Marchetti, J.-F. Joanny, S. Ramaswamy, T. B. Liverpool, J. Prost, M. Rao, and R. A. Simha, Hydrodynamics of soft active matter, Rev. Mod. Phys. **85**, 1143 (2013).

[30] A. P. Solon, Y. Fily, A. Baskaran, M. E. Cates, Y. Kafri, M. Kardar, and J. Tailleur, Pressure is not a state function for generic active fluids, Nat. Phys. **11**, 673 (2015).

[31] S. C. Takatori and J. F. Brady, Forces, stresses and the (thermo?) dynamics of active matter, Curr. Opin. Colloid Interface Sci. **21**, 24 (2016).

[32] I. Petrelli, L. F. Cugliandolo, G. Gonnella, and A. Suma, Effective temperatures in inhomogeneous passive and active bidimensional Brownian particle systems, Phys. Rev. E **102**, 012609 (2020).

[33] L. Ortlieb, S. Rafaï, P. Peyla, C. Wagner, and T. John, Statistics of Colloidal Suspensions Stirred by Microswimmers, Phys. Rev. Lett. **122**, 148101 (2019).

[34] J. Palacci, C. Cottin-Bizonne, C. Ybert, and L. Bocquet, Sedimentation and Effective Temperature of Active Colloidal Suspensions, Phys. Rev. Lett. **105**, 088304 (2010).

[35] M. Han, J. Yan, S. Granick, and E. Luijten, Effective temperature concept evaluated in an active colloid mixture, Proc. Natl. Acad. Sci. USA **114**, 7513 (2017).

[36] A. Kaiser, H. H. Wensink, and H. Löwen, How to Capture Active Particles, Phys. Rev. Lett. **108**, 268307 (2012).

[37] H. H. Wensink and H. Löwen, Aggregation of self-propelled colloidal rods near confining walls, Phys. Rev. E **78**, 031409 (2008).

[38] N. Nikola, A. P. Solon, Y. Kafri, M. Kardar, J. Tailleur, and R. Voituriez, Active Particles with Soft and Curved Walls: Equation of State, Ratchets, and Instabilities, Phys. Rev. Lett. **117**, 098001 (2016).

[39] Y. Fily, A. Baskaran, and M. F. Hagan, Dynamics of self-propelled particles under strong confinement, Soft Matter **10**, 5609 (2014).

[40] G. Junot, G. Briand, R. Ledesma-Alonso, and O. Dauchot, Active versus Passive Hard Disks against a Membrane: Mechanical Pressure and Instability, Phys. Rev. Lett. **119**, 028002 (2017).

[41] G. D'Anna, P. Mayor, A. Barrat, V. Loreto, and F. Nori, Observing Brownian motion in vibration-fluidized granular matter, Nature (London) **424**, 909 (2003).

[42] H. Turlier, D. A. Fedosov, B. Audoly, T. Auth, N. S. Gov, C. Sykes, J.-F. Joanny, G. Gompper, and T. Betz, Equilibrium physics breakdown reveals the active nature of red blood cell flickering, Nat. Phys. **12**, 513 (2016).

[43] T. Betz, M. Lenz, J.-F. Joanny, and C. Sykes, Atp-dependent mechanics of red blood cells, Proc. Natl. Acad. Sci. USA **106**, 15320 (2009).

[44] E. Ben-Isaac, Y. K. Park, G. Popescu, F. L. H. Brown, N. S. Gov, and Y. Shokef, Effective Temperature of Red-Blood-Cell Membrane Fluctuations, Phys. Rev. Lett. **106**, 238103 (2011).

[45] R. Kubo, M. Toda, and N. Hashitsume, *Statistical Physics II: Nonequilibrium Statistical Mechanics*, Vol. 31 (Springer Science & Business Media, Berlin, 2012).

[46] L. Giomi, N. Hawley-Weld, and L. Mahadevan, Swarming, swirling and stasis in sequestered bristle-bots, Proc. R. Soc. A: Math., Phys. Eng. Sci. **469**, 20120637 (2013).

[47] See Supplemental Material at http://link.aps.org/supplemental/10.1103/PhysRevResearch.4.L042006 for experimental details and additional results as well as a theoretical analysis of the experiments. Two supplementary movies are provided SMovie1 (at 100 fps using 31 robots) and SMovie2 (at 250 fps using 61 robots).

[48] O. Hallatschek, E. Frey, and K. Kroy, Tension dynamics in semiflexible polymers. I. Coarse-grained equations of motion, Phys. Rev. E **75**, 031905 (2007).

[49] Z. Zhang, Y. Wang, Y. Amarouchene, R. Boisgard, H. Kellay, A. Würger, and A. Maali, Near-Field Probe of Thermal Fluctuations of a Hemispherical Bubble Surface, Phys. Rev. Lett. **126**, 174503 (2021).

[50] A. Maali, C. Hurth, R. Boisgard, C. Jai, T. Cohen-Bouhacina, and J.-P. Aimé, Hydrodynamics of oscillating atomic force microscopy cantilevers in viscous fluids, J. Appl. Phys. **97**, 074907 (2005).

[51] A. Clerk, Quantum-limited position detection and amplification: A linear response perspective, Phys. Rev. B **70**, 245306 (2004).

[52] A. A. Clerk, M. H. Devoret, S. M. Girvin, F. Marquardt, and R. J. Schoelkopf, Introduction to quantum noise, measurement, and amplification, Rev. Mod. Phys. **82**, 1155 (2010).